AD/A-003 012

STRENGTH-SIZE RELATIONSHIPS IN CERAMIC MATERIALS: INVESTIGATION OF PYROCERAM 9606

G. K. Bansal, et al

Battelle Columbus Laboratories

Prepared for:

Office of Naval Research

November 1974

Security Classification

AD/A003012

DOCUMENT CONTROL DATA - R & D

(Security classification of title, body of abstract and indexing annotation must be entered when the overall report is classified)

1. ORIGINATING ACTIVITY (Corporate author)	2a. REPORT SECURITY CLASSIFICATION
Battelle, Columbus Laboratories 505 King Avenue, Columbus, Ohio, 43201	Unclassified
	2b. GROUP None

3. REPORT TITLE

Strength-Size Relationships in Ceramic Materials:
Investigation of Pyroceram 9606

4. DESCRIPTIVE NOTES (Type of report and inclusive dates)

Technical Report No. 3

5. AUTHOR(S) (First name, middle initial, last name)

Bansal, G. K., Duckworth, W. H., and Niesz, D. E.

6. REPORT DATE	7a. TOTAL NO. OF PAGES	7b. NO. OF REFS
November, 1974	~~33~~ 38	3

8a. CONTRACT OR GRANT NO.	9a. ORIGINATOR'S REPORT NUMBER(S)
N00014-73-C-0408, NR 032-541	
b. PROJECT NO.	3
c.	9b. OTHER REPORT NO(S) (Any other numbers that may be assigned this report)
d.	2

10. DISTRIBUTION STATEMENT

Reproduction in whole or in part is permitted for any purpose of the United States Government.

11. SUPPLEMENTARY NOTES	12 SPONSORING MILITARY ACTIVITY
—	Office of Naval Research Department of Navy

13. ABSTRACT

This research was directed to characterizing and explaining strength-size relationships exhibited by ceramic materials. Precise measurements of the strength of the commercial glass-ceramic, Corning's Pyroceram 9606, are reported. Fracture stresses in specimens differing in each linear dimension by a factor of five were measured at room temperature under carefully controlled conditions which minimized subcritical crack growth. Data obtained were analyzed with the aid of fractographic examinations to determine applicability of various size-effect theories. Findings indicated validity of the spurious-effect theory, and that the strength of Pyroceram 9606 can be described adequately in terms of stress alone. Maximum tensile stress criteria for failure were determined.

(38)

DD FORM 1 NOV 65 1473

Security Classification

14. KEY WORDS	LINK A		LINK B		LINK C	
	ROLE	WT	ROLE	WT	ROLE	WT
Ceramic Strength Behavior						
Size-Strength Relations						
Brittle Fracture						
Critical Flaw Size						
Fracture Energy						
Strength Theories						

ABSTRACT

This research was directed to characterizing and explaining strength-size relationships exhibited by ceramic materials. Precise measurements of the strength of the commercial glass-ceramic, Corning's Pyroceram 9606, are reported. Fracture stresses in specimens differing in each linear dimension by a factor of five were measured at room temperature under carefully controlled conditions which minimized subcritical crack growth. Data obtained were analyzed with the aid of fractographic examinations to determine applicability of various size-effect theories. Findings indicated validity of the spurious-effect theory, and that the strength of Pyroceram 9606 can be described adequately in terms of stress alone. Maximum tensile stress criteria for failure were determined.

STRENGTH-SIZE RELATIONSHIPS IN CERAMIC MATERIALS: INVESTIGATION OF PYROCERAM 9606

by

G. K. Bansal, Winston Duckworth, and D. E. Niesz

Table of Contents

List of Tables

List of Figures

SUMMARY AND CONCLUSIONS

The uniaxial strength of the glass-ceramic, Corning's Pyroceram 9606, with respect to specimen size has been determined from precise measurements at room temperature under controlled conditions which minimized subcritical crack growth. The measurements coupled with fractographic examinations revealed the following:

(1) Fracture originated from tension at either of two sites:
   (a) At the surface in which case fractography was unremarkable.
   (b) At an internal pore approximately 80 μm in diameter.
(2) The critical stress at the fracture site differed depending on whether fracture was from a surface or pore origin.
(3) For both surface and pore origins, the fracture stress was independent of specimen size. Specimens differing in each linear dimension by a factor of five were evaluated.
(4) Material from two billets of Pyroceram 9606 exhibited different average fracture-stress values, as follows:

	Billet A	Billet B
Surface Origin	45.0 ksi	57.1 ksi
Pore Origin	35.8 ksi	39.5 ksi

We conclude from these results that a simple maximum tensile stress criterion should be used to describe the strength of Pyroceram 9606 for structural design purposes. If the pores were not present, no failure should be observed when tensile stresses are maintained below the values given above for surface origins. Elimination of the pores might be accomplished by processing refinements.

A conservative maximum tensile stress criterion that would account for the "worst" case of pore origin is the fracture stress when one of the 80 μm pores would happen to lie immediately below a critical surface crack. In this case, the calculated fracture stress is 30.0 ksi for Billet B material and 26.0 ksi for Billet A material. No failure would be expected if imposed tensile stresses are maintained below these values.

The research findings indicate validity of the spurious-effect theory of the observed size dependence of ceramic strengths, primarily because no size dependence of critical stress was found. The skin-effect theory also is rejected because no size dependence of Young's modulus was found. Of perhaps greater significance, spurious effects associated with conventional treatment of the data were revealed that would cause an apparent size effect and misleading scatter in strength values assigned to Pyroceram 9606.

This latter finding suggests that inadequacies in the quality of available strength data are more responsible than true strength behavior of ceramic materials in assigning credibility to statistical theories. As implied above, there was no substantial evidence in the data obtained which supports the contention of statistical theories that fracture at any stress must be treated as an inherently probabilistic event in defining a failure criterion.

Since the stored-strain-energy theory requires subcritical crack growth for its prediction of a size effect and the data at hand were obtained under conditions which minimized such growth, this theory should be considered as untested at this time. Future plans include assessment of its validity.

Estimated values of fracture-mechanics parameters for Pyroceram 9606 were obtained incidental to the investigation of strength-size relationships as follows

	Billet A	Billet B
Fracture energy, J/m^2	20.1	24.5
Critical surface crack depth, μm	40	30
Critical stress-intensity factor, $MNm^{-3/2}$	2.14	2.36

INTRODUCTION

A central problem in structural designing with brittle materials results from an observed size dependence of fracture stress and a related stress-distribution dependency. With a size dependence, strength obviously cannot be described for structural design purposes in terms of stress alone, but no alternative failure criterion which correctly accounts for the size effect has been established for any brittle material.

This report covers an investigation and analysis of the strength of Pyroceram 9606, a glass-ceramic material produced by Corning Glass Works which is used by the Navy for radomes. The investigation constitutes one phase of an ONR project at Battelle to define and explain strength-size relationships exhibited by ceramics of interest for Navy structural applications, so that the applicable failure criterion for each can be specified.

Different explanations for the observed size effect (and different failure criteria) have been proposed in the following theories:

- Spurious-effect theory
- Statistical theories
- Skin-effect theory
- Stored-strain-energy-effect theory.

The project objectives include finding which, if any, of these theories applies to each selected ceramic.

The spurious-effect theory is often used implicitly in accounting for variations among reported strengths of a brittle material. According to this theory, there is no real size effect and observed differences in strengths from one specimen size to another result from variability in stress-measurement errors and/or in the specimen material, including its surface character. The theory suggests that a brittle material would exhibit a unique value of fracture stress independent of specimen size if these sources of variability are eliminated.

The widely accepted statistical theories, of which Weibull's[1]* is most prominent, contend that fracture at any stress should be considered as probabilistic rather than fixed. From this viewpoint, special significance is attached to the dispersion of values in a single set of strength data--an intrinsic dispersion is assumed which constitutes, in effect, a strength characteristic of the material. The theories provide expressions for the probability of fracture as a function of stress derived on the basis the material contains a random flaw population and breaks at the most-severe flaw like a chain at its weakest link. Because there is apt to be a more severe flaw among the greater number of flaws in a large than a small specimen,

---

* References are listed on page 33.

a size effect is predicted with small specimens appearing stronger. The strength of a material is characterized from the statistical probability expressions by empirically determined material parameters, such as σ_u, σ_o, and m in the following Weibull expression:

$$P_f = 1 - \exp\left[-V\left(\frac{\sigma-\sigma_u}{\sigma_o}\right)^m\right]$$

where: P_f = probability of fracture

V = stressed volume

σ = applied stress.

Although less obvious than in the case of the spurious-effect theory, the statistical theories place extraordinary demands on the quality of strength data. Values in a set of data must reflect only the assumed intrinsic dispersion free of effects from lack of control in strength testing or specimen preparation.

In the skin-effect theory,[2] the material is characterized as a layered composite having a skin of invariant thickness whose Young's modulus differs from that of the underlying material. The strength of such a composite will approach the skin strength for very small specimens and the substrate strength for very large specimens; the relation between strength and specimen size being derived readily from elementary principles of mechanics. If this theory is valid, Young's modulus as well as strength is size dependent.

A relatively new theory advanced by Glucklich[3] requires subcritical crack growth prior to catastrophic fracture, and proposes that the energy consumed in such growth can affect strength to an extent dependent on the total available stored strain energy. Since strain energy stored in a stressed

specimen is proportional to the specimen volume, higher stress levels will be required to fracture small than large specimens (i.e., to obtain the necessary condition of sufficient stored strain energy for propagation of the critical crack). Strain energy is stored in the load train and the testing machine as well as in the specimen, so specimen size is not the only factor which might affect measured strengths as a consequence of subcritical crack growth. Because of the large amount of stored strain energy available with dead-weight loading, for example, Glucklich's theory would predict little size dependence when specimens are loaded in this manner.

The research efforts described in the pages which follow were addressed primarily to the question of whether the strength of Pyroceram 9606 exhibits a real size depencence. Emphasis was placed on precision in strength measurements and on experimental control in specimen preparation and testing. Fractography was utilized for interpreting results.

MATERIAL AND SPECIMEN PREPARATION

The glass-ceramic material investigated, Corning Glass Works' Pyroceram 9606, is reported to be made from a magnesium aluminosilicate glass containing titania as a nucleating agent, and cordierite ($2MgO \cdot 2Al_2O_3 \cdot 5SiO_2$) is reported to be the major crystalline phase in the material.[4] Two blanks or billets, 5 x 10 x 1-1/4 in., of the material were prepared specially by Corning for the investigation. Both were cast from the same glass melt, and in the crystallization process each billet was subjected to the same heat treatment.

Optical microscopy, however, revealed the two billets had different microstructures, necessitating separate strength analyses of each and limiting the number of replicate specimens for strength determinations. Figure 1 presents micrographs of chemically etched sections from each billet showing a nonuniform microstructure in Billet A and a relatively uniform microstructure in Billet B. Billet A contained occasional large crystals which were absent in Billet B.

The microstructural differences were not reflected in Young's modulus data, indicating there was little variation in phases present. Young's modulus values were obtained from a number of bend- and compression-test specimens from each billet. The maximum variation in these values was less than two percent. Included were data from specimens taken from two orientations within a billet. Measured values of Young's modulus are reported in a later section; the average value was 16.6×10^6 psi.

The two sizes of specimens* shown in Figure 2 were used for strength measurements. The larger specimen had each linear dimension five times that of the smaller one; the volume and area ratios are 125 and 25, respectively. The billets were diamond cut and ground to obtain these specimens. Standard diamond sawing techniques using specified infeeds, table speeds, and coolant were used for cutting. Each specimen was cut oversize so that approximately 0.05 in. remained for removal from all surfaces by surface grinding. Coarse grinding was done with a 120-grit, metal-bonded diamond wheel of Type MDA-S under the following conditions:

---

* (0.2 x 0.1 x 1.5 in. and 1.0 x 0.5 x 7.5 in.)

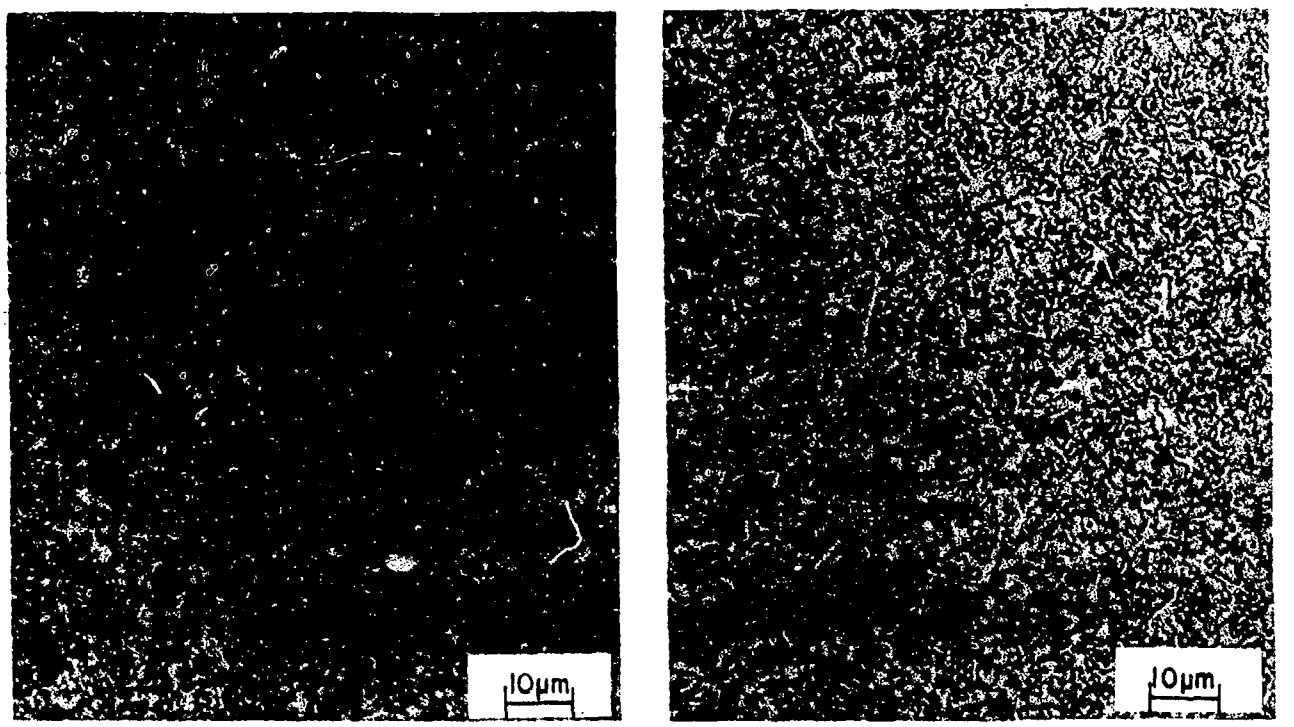

Billet A

Billet B

FIGURE 1. OPTICAL MICROGRAPHS, POLISHED SECTIONS ETCHED WITH 5% HF SOLUTION

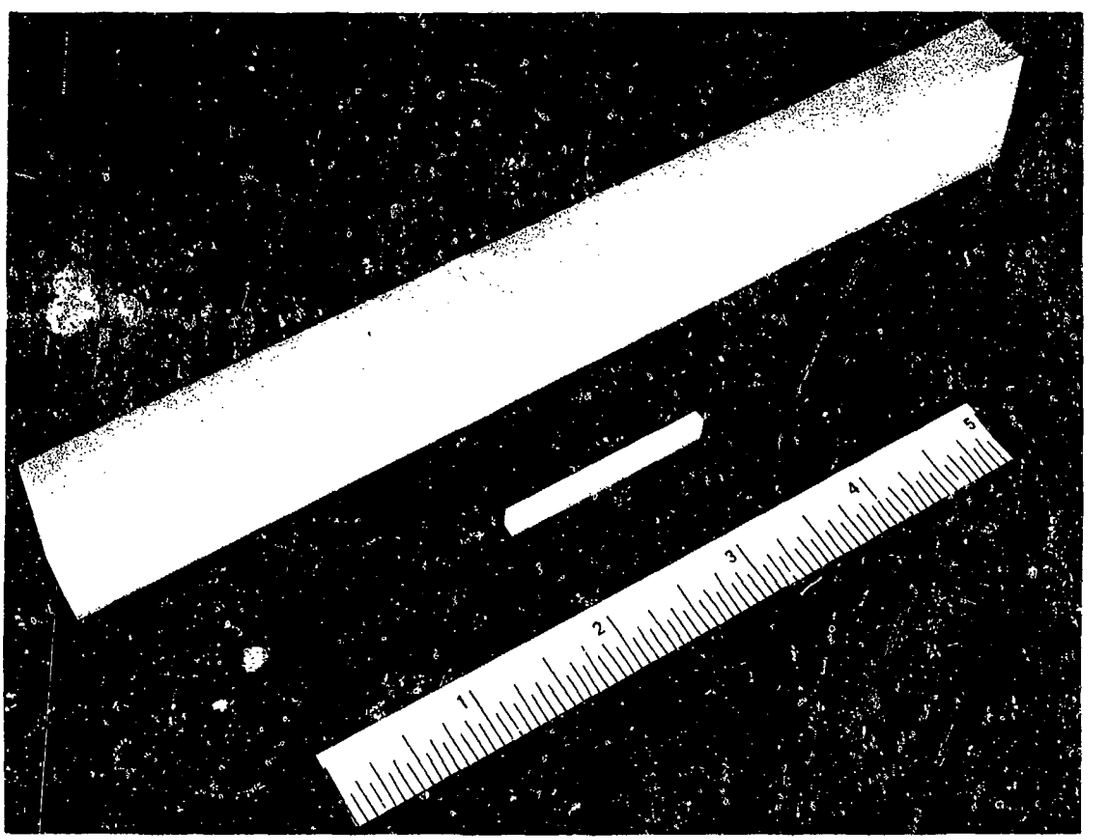

FIGURE 2. STRENGTH SPECIMENS

Wheel dimensions	7-in. diameter, 1/2 in. wide
Bond depth	1/4 in.
Diamond concentration	100
Wheel speed	5500 rpm
Table speed	1 ft/min
Depth of cut	0.001 in./pass
Cross feed	0.06 in. per table reversal
Coolant	Water with rust inhibitor

The final 0.01 in. was removed with a 320-grit diamond wheel using an infeed of 0.0005 in./pass and other conditions as listed above. Edges were rounded slightly by polishing with 1 μm diamond paste to eliminate edge-initiated fractures.

Specimens were degreased in trichloroethylene, washed with detergent, water, and acetone, and then were dried at 125 C [257 F]. After drying, specimens were stored in vacuum until tested.

STRENGTH TESTING PROCEDURE

Strengths were measured in four-point bending. In measuring strengths, we employed a special bend-test fixture, specimen dimensional ratios, span lengths, and procedures developed earlier in the project to eliminate spurious stresses from wedging, unequal moments, twisting, and frictional forces.[5] By these means, errors in stress measurements were found to be reduced to the order of 1 percent. Figure 3 is a schematic of the bend-test fixture.

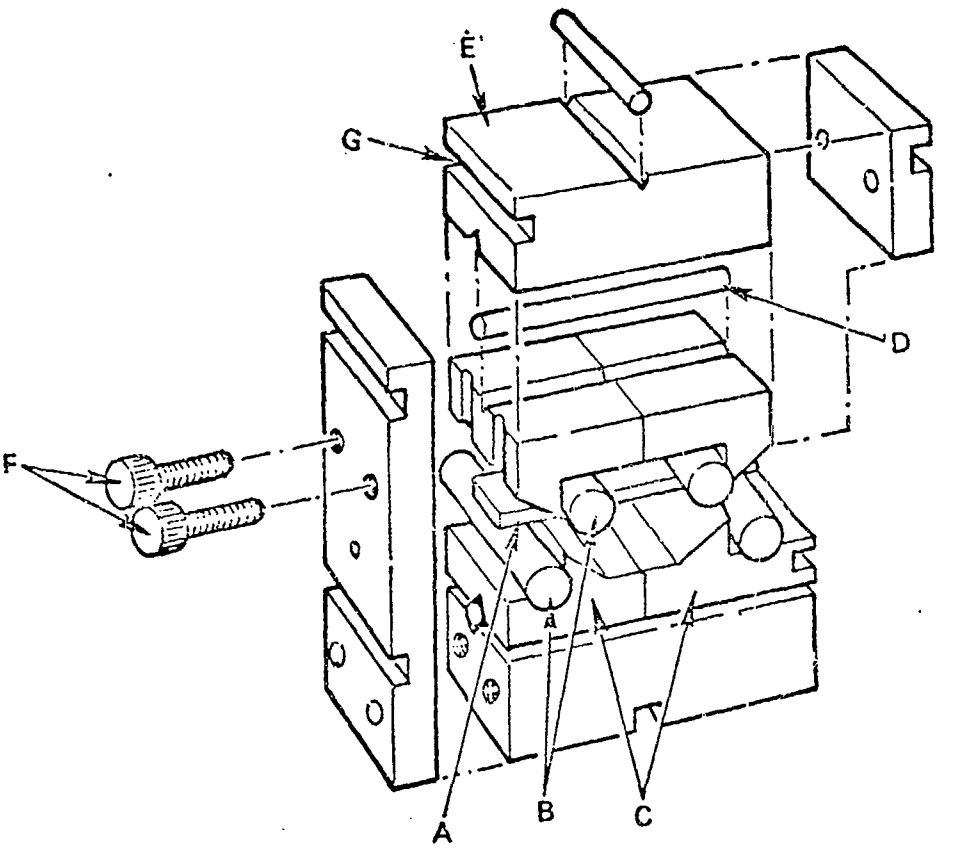

FIGURE 3. SCHEMATIC OF BEND FIXTURE

Note: The specimen at A is loaded via the hardened steel rollers, B. Independently rotable hardened steel ways (the lower pair indicated at C) support the rollers and are free to pivot about bearings one of which is indicated at D. The bearings rest in V-grooves in the ways and in pillow blocks, e.g., E. The position of the upper span relative to the lower span can be adjusted by means of the screws at F and the various elements of the fixture are located at the onset of the test by rubber bands which are held in several slots, one being indicated at G.

Stress, σ, in the bend specimens was calculated using the simple beam expression, $\sigma = Mc/I$, where M is the applied moment, c is the distance to the neutral axis, and I is the cross-sectional moment of inertia. Error is introduced in stress values obtained from this expression if the material exhibits nonlinear stress-strain behavior or different values of Young's modulus in tension and compression. Pyroceram 9606 was found to exhibit neither in experiments described in the next section of the report.

Preliminary bend-strength tests were conducted on small specimens from an uncharacterized billet of Pyroceram 9606 to establish test conditions which minimized static fatigue, a phenomenon caused by subcritical crack growth. The specimens were tested in dry nitrogen (< 3 ppm water) at each of four strain rates. Strength data obtained are summarized in Table 1, and representative load-time curves are plotted in Figure 4.

TABLE 1. STRAIN-RATE SENSITIVITY OF PYROCERAM 9606

Cross-head Speed, in./min.	Stress Rate, ksi/sec	Average Fracture Stress,[(a)] ksi(MNm^{-2})	Coefficient of Variation, percent
0.002	0.2	39.4 (272)	1.36
0.01	1.0	42.8 (295)	1.32
0.1	10.0	43.0 (296)	2.34
0.2	20.0	43.1 (297)	2.00

(a) Average of four values in each case.

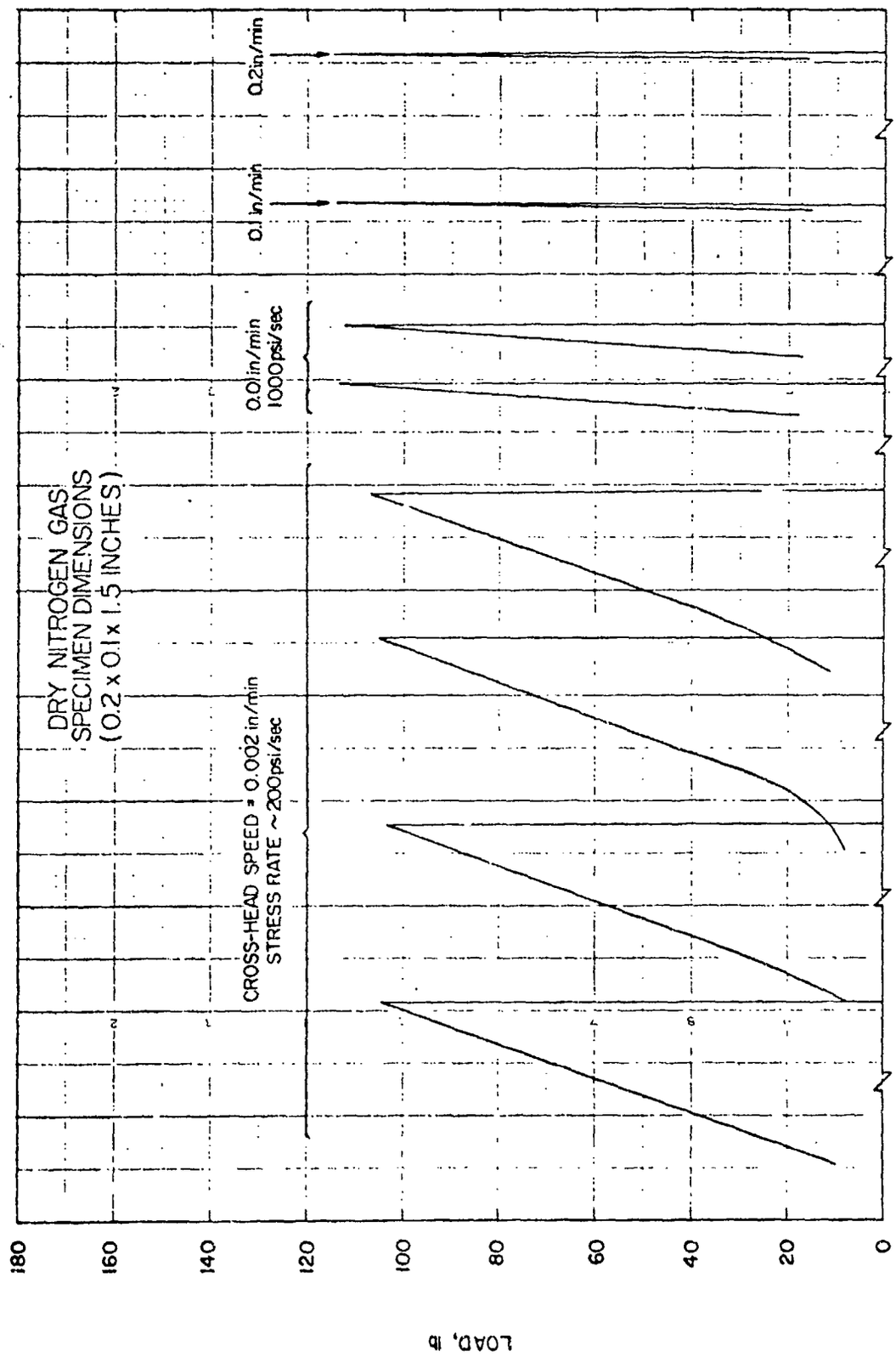

FIGURE 4. REPRESENTATIVE LOAD-TIME CURVES

As shown in Table 1, strengths increased with increasing strain rate. However, with cross-head speeds between 0.1 and 0.2 in./minute corresponding to 10,000 and 20,000 psi/second, no appreciable increase in strength was observed. Therefore, a cross-head speed equivalent to $\sim$ 15,000 psi/second [100 MNm^{-2}/second] was selected for strength measurements.

YOUNG'S MODULUS DETERMINATIONS

Values of Young's modulus were obtained from direct-compression tests on specimens of two sizes, 0.2 x 0.2 x 0.8 and 1.0 x 1.0 x 4.0 in., in normal laboratory air at room temperature. Each specimen was loaded parallel to the length direction, and axial strain in each of its four faces at midlength was measured with resistance strain gages. The average strain value from the four gages as a function of applied stress was used to calculate Young's modulus.

Table 2 gives the values obtained. The billet cutting plans shown in Figures 5 and 6 give the locations in each billet from which the specimens in Table 2 were taken.

As mentioned previously, the Young's modulus data indicate no difference in elastic behavior between the materials in Billets A and B and in the material within each billet. The data also indicate that Young's modulus is independent of specimen size. Accordingly, the skin-effect theory does not appear applicable to Pyroceram 9606.

TABLE 2. YOUNG'S MODULUS DATA FOR PYROCERAM 9606

Specimen Size, inches	Specimen Identification	Young's Modulus 10^6 psi [GNm^{-2}]
	BILLET A	
Large - 1.0 x 1.0 x 4.0	AC-1	16.55
	AC-2	16.45
		Average 16.50 [113.76]
	AC-3	16.59 [115.07]
Small - 0.2 x 0.2 x 0.8	AC-4	16.69
	AC-5	16.51
		Average 16.60 [114.45]
	BILLET B	
Large - 1.0 x 1.0 x 4.0	BC-1	16.54
	BC-2	16.62
		Average 16.58 [114.32]
Small - 0.2 x 0.2 x 0.8	BC-3	16.74
	BC-4	16.48
		Average 16.61 [114.52]

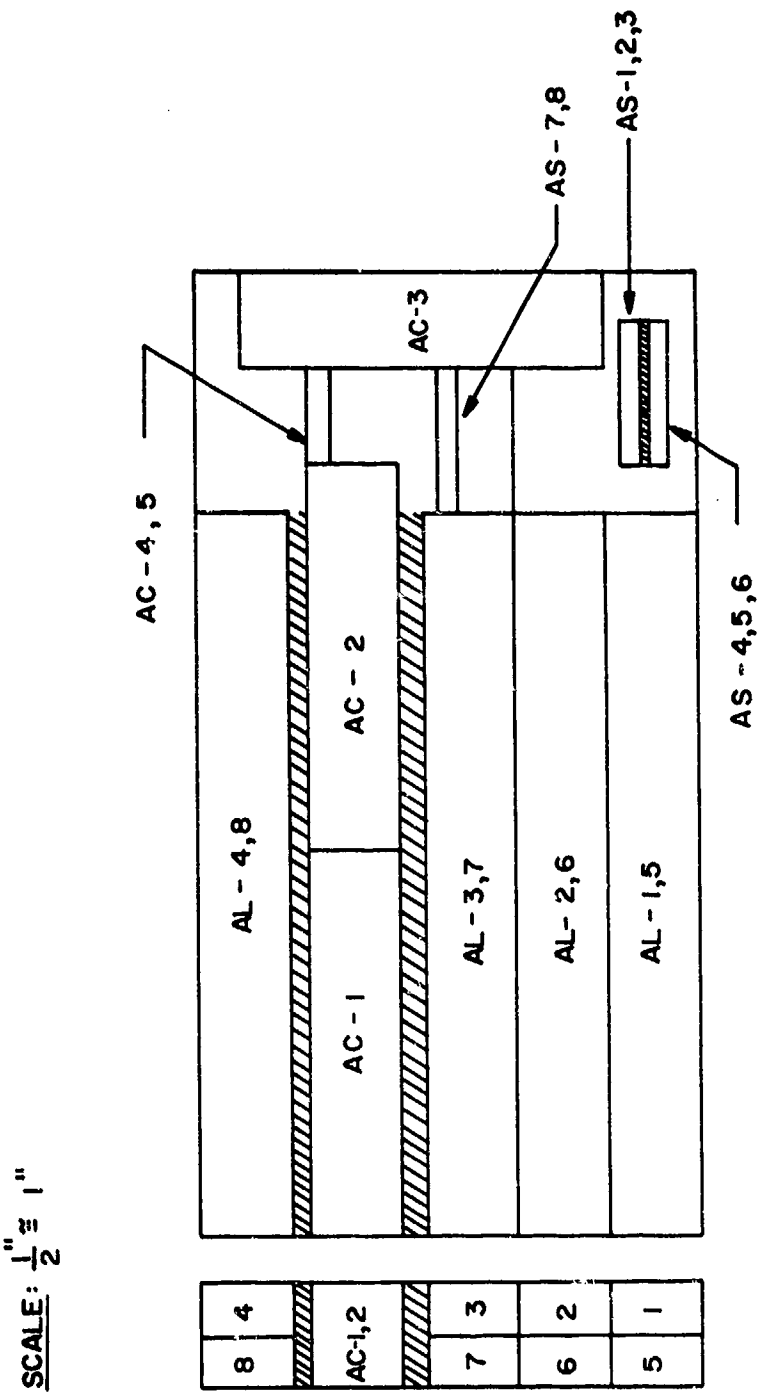

SCALE: $\frac{1}{2}" \equiv 1"$

FIGURE 5. BILLET-A CUTTING PLAN

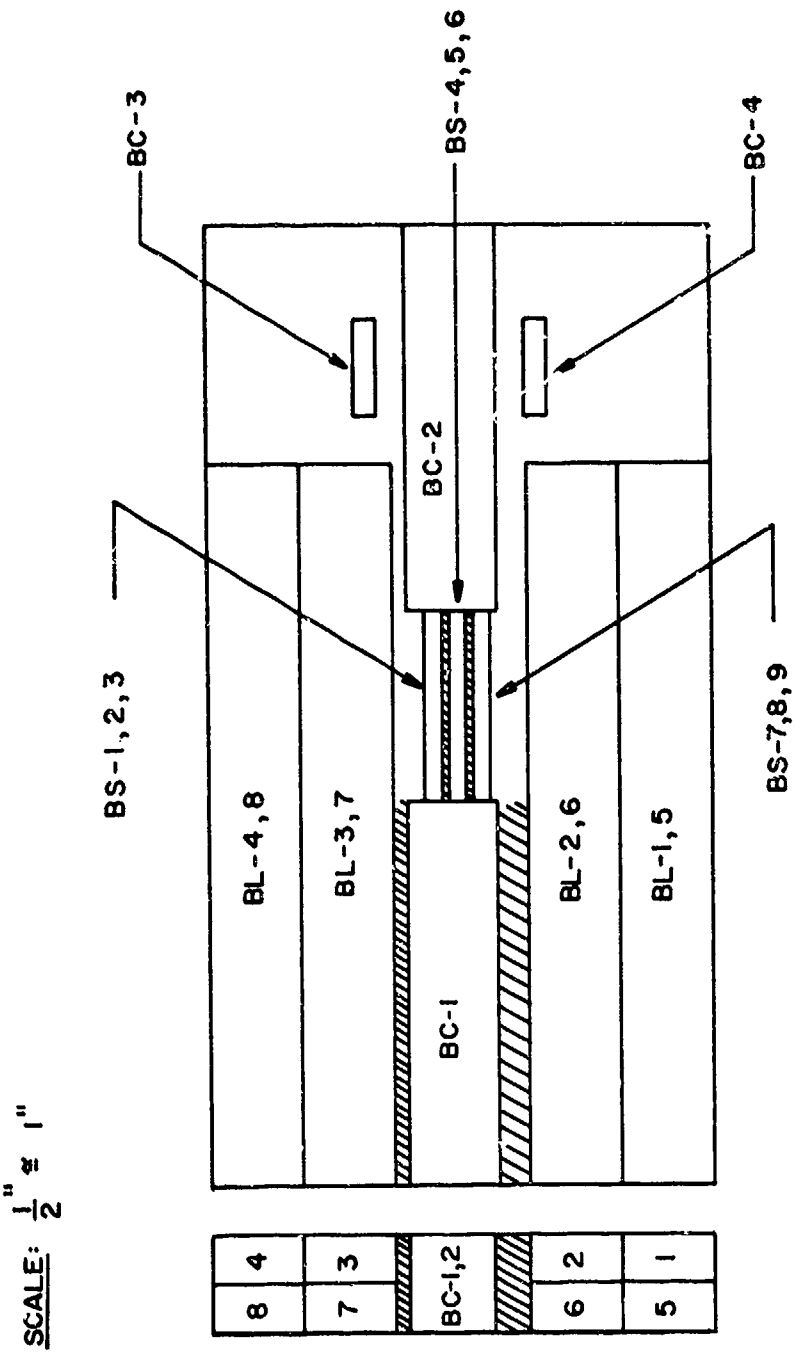

FIGURE 6. BILLET-B CUTTING PLAN

Young's modulus also was assessed from data obtained in bend tests on several specimens. Axial strains in both the tension and compression surfaces were measured with resistance strain gages as a function of the applied moment. The curves were linear to failure. Moduli values from compression-surface strains were within the range of those in Table 2 from the direct-compression tests. Moduli values from tensile strains were about 1 percent less than those from compressive strains when measured on the same specimen. As pointed out earlier, these findings indicate that little or no error is introduced from using the simple beam expression to determine stresses in bend specimens.

STRENGTH-TEST RESULTS

Fractography

Before presenting the strength-size data, the nature of fracture-initiation sites found in Pyroceramic 9606 will be described. After strength testing, each specimen was subjected to fractography using both optical and scanning electron microscopy.

No differences were found in the nature of fracture-initiation sites attributable to billet-to-billet variation; the fractographic findings were similar in specimens from the two billets.

Figure 7 shows fractures originating from subsurface pores approximately 80 μm in diameter. The maximum stress in specimens which failed at these pores varied depending on the distance of the pore from the tensile surface. However, the stress at the pore site at fracture was

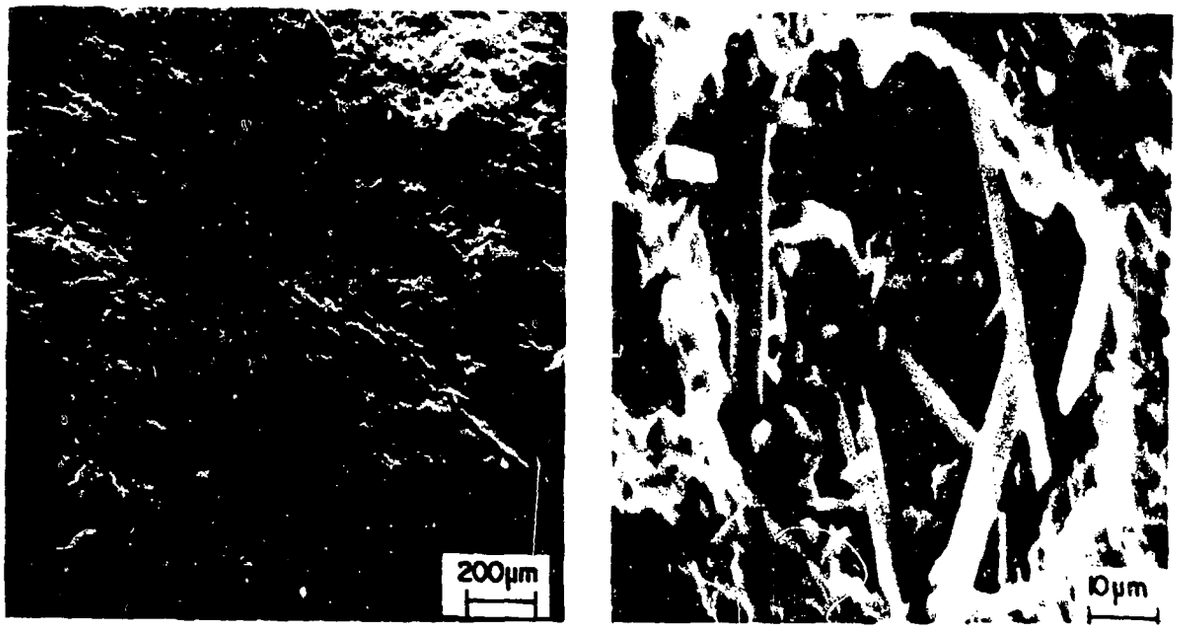

Specimen BL-4

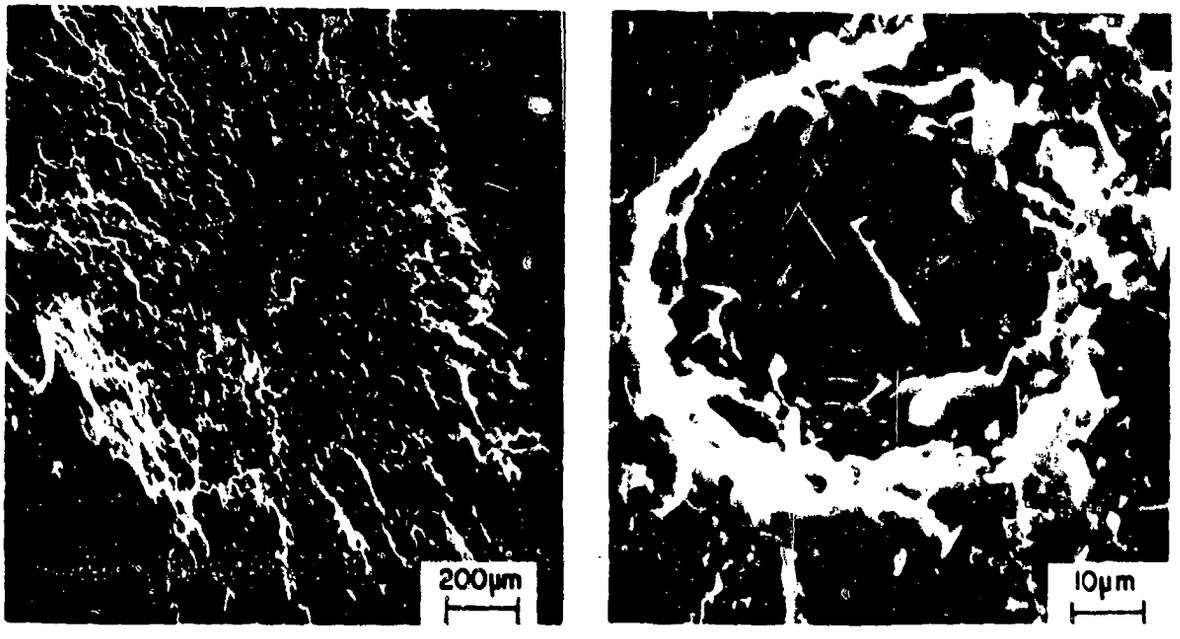

Specimen BL-3

FIGURE 7. SCANNING ELECTRON MICROGRAPHS OF INTERNAL PORE FRACTURE SITES

invariably ∿35.8 ksi [247 MNm^{-2}] in specimens from Billet A and ∿39.5 ksi [272 MNm^{-2}] in specimens from Billet B. A fibrous structure was always associated with these pores.

Figure 8 shows fracture initiation at the surface where no obvious flaw was detected. Specimens failing at the surface always had higher strengths than those failing at internal pores.

In a few large specimens, edge-initiated failure (Figure 8, Specimen BL-7) occurred due to insufficient rounding of the specimen edges. Specimens failing from edges had the lowest fracture stresses observed. The values were considered spurious and were not used in strength analyses.

Figure 9 shows the fracture surface of Specimen BL-2 which had a pore 30 μm in diameter so close to the tensile surface that the ligament between the pore and the surface fractured prior to catastrophic failure to produce a surface flaw slightly larger than the pore diameter.

Strength-Size Data

Table 3 gives the measured strengths of specimens of both sizes from each billet. The billet cutting plans in Figures 5 and 6 identify the location from which each specimen was taken. As pointed out earlier, microstructures of material in each billet differed, and this is reflected in the strength levels. Because the materials were not alike, strength data from the two billets have been analyzed separately.

The data in Table 3 show that fracture stress was dependent on whether fracture initiated at the surface or at an internal pore. Most of the small specimens failed at the surface, while the failure origins in

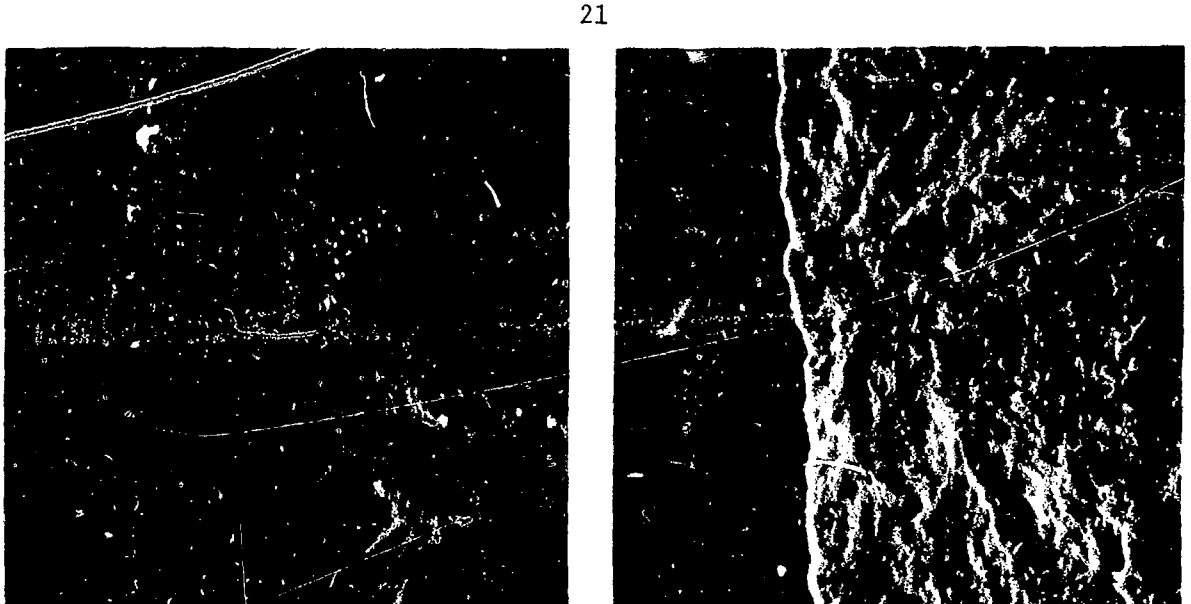

Specimen BS-2

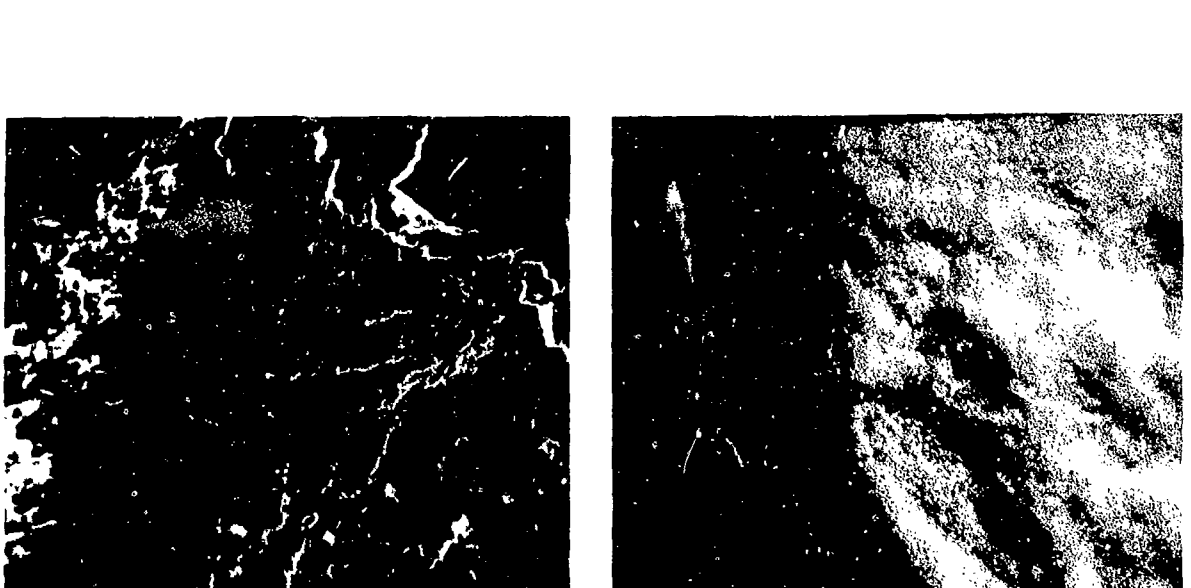

Specimen BS-4 Specimen BL-7

FIGURE 8. SURFACE FRACTURE SITES (SCANNING ELECTRON MICROGRAPHS OF SPECIMENS BS-2 and BS-4 AND OPTICAL MICROGRAPH OF SPECIMEN BL-7)

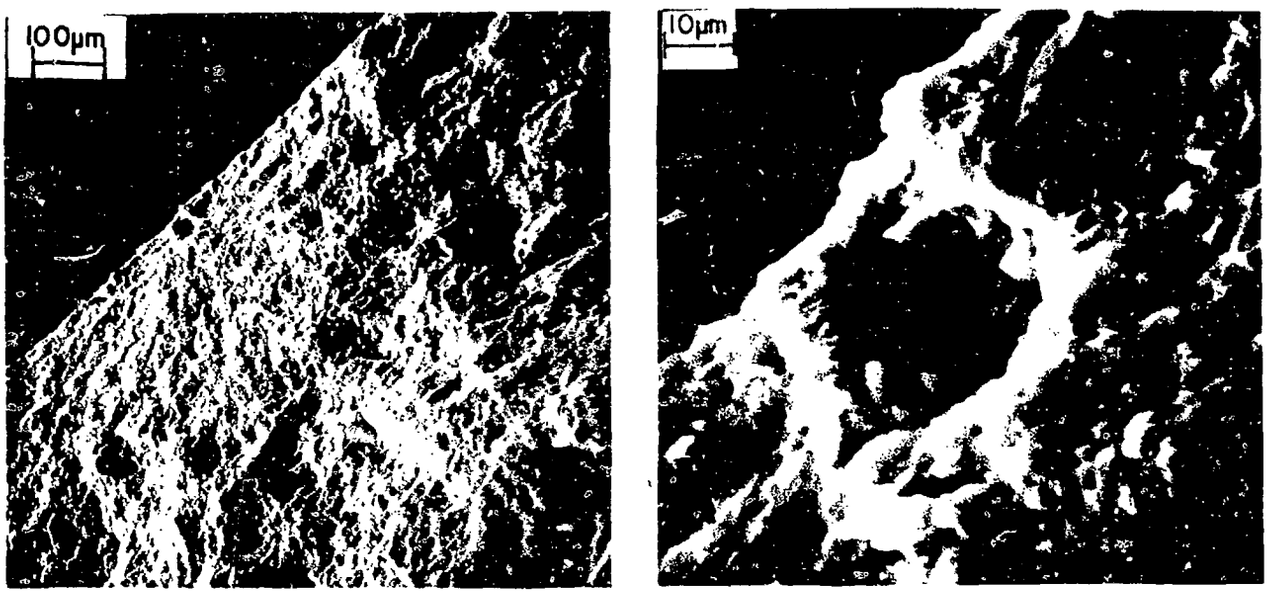

Specimen BL-2

FIGURE 9. SCANNING ELECTRON MICROGRAPHS OF SURFACE PORE FRACTURE SITE

TABLE 3. STRENGTH-SIZE DATA ON PYROCERAM 9606

Specimen Identification	Fracture Site	Stress at Fracture, psi [MNm^{-2}] At Surface	At Fracture Site
	BILLET A		
	Small Specimens		
AS-1	Surface	46,125 [318]	---
AS-2	Surface	45,750 [315]	---
AS-3	Surface	43,690 [301]	---
AS-4	Surface	43,875 [303]	---
AS-5	Surface	44,625 [308]	---
AS-6	Surface	42,750 [295]	---
AS-7	Surface	45,375 [313]	---
AS-8	Pore	35,250 [243]	35,000 [241]
Average:	Surface	44,600 [308]	
Coefficient of Variation (Surface)		2.5%	
	Large Specimens		
AL-1	Corner	38,650 [266]	---
AL-2	Surface	44,450 [306]	---
AL-3	Corner	34,000 [234]	---
AL-4	Pore	38,500 [265]	37,500 [259]
AL-5	Surface	45,300 [312]	---
AL-6	Surface	48,300 [333]	---
AL-7	Corner	36,175 [249]	---
AL-8	Pore	35,500 [245]	35,000 [241]
Average:	Surface	46,000 [317]	---
	Pore	37,000 [255]	36,250 [250]
	BILLET B		
	Small Specimens		
BS-1	Surface	59,050 [407]	---
BS-2	Surface	52,500 [362]	---
BS-3	Surface	58,875 [406]	---
BS-4	Surface	60,375 [416]	---
BS-5	Pore	47,250 [326]	40,500 [279]
BS-6	Surface	58,125 [401]	---
BS-7	Surface	55,125 [380]	---
BS-8	Surface	58,500 [403]	---
BS-9	Surface	56,250 [388]	---
Average:	Surface	57,350 [395]	
Coefficient of Variation (Surface)		4.2%	
	Large Specimens		
BL-1	Surface	54,750 [378]	---
BL-2	Surface Pore[a]	55,500 [383]	---
BL-3	Pore	42,375 [292]	38,700 [267]
BL-4	Pore	45,750 [315]	39,500 [272]
BL-5	Surface	57,375 [396]	---
BL-6	Corner	38,625 [266]	---
BL-7	Corner	34,125 [235]	---
BL-8	Pore	40,875 [282]	39,300 [271]
Average:	Surface	56,060 [387]	---
	Pore	43,000 [296]	39,170 [270]

(a) Excluded in calculating average.

large specimens were about equally distributed between surface and internal pore sites.

Fracture initiated at the surface in 20 of the 28 specimens whose strengths were determined. When this occurred, strength appeared to be independent of specimen size suggesting validity of the spurious-effect theory. Average fracture stresses of the large and small specimens exhibiting surface failures were as follows:

	Average Fracture Stress, ksi	
Specimen Size	Billet A	Billet B
Small	44.6	57.4
Large	46.0	56.1

The dispersion of values included in each of the above averages was quite small. Coefficients of variation were, respectively, 2.5 and 4.2 percent for 7 and 8 small specimens from Billets A and B; for large specimens the maximum variation of an individual value from the average fracture-stress value was less than 5 percent.

On the basis of these data, in the absence of pore-initiated failure a simple maximum tensile stress criterion would adequately define the strength of Pyroceram 9606 for structural design purposes. Under the particular conditions of surface finish, strain rate, and environment used, no fracture should occur when surface tensile stresses are maintained below the following indicated values:

Billet A -- 45.0 ± 1.1 ksi

Billet B -- $57.1 + 1.7$ ksi

(95% confidence limits are shown)[6]

The fact that most of the small specimens exhibited surface failures but about equal numbers of large specimens failed at the surface and internal-pore sites is attributed to (1) a sparse pore population making it less likely one will be present in a small specimen and (2) the need for a pore to reside nearer the surface in a small specimen for it to experience sufficient stress to compete with potential surface origins under higher stress, the stress gradient being steeper in the small specimens.

From Table 3, critical tensile stresses at the fracture sites in the seven specimens exhibiting internal pore origins were as follows:

	Fracture Stress, ksi	
Specimen Size	Billet A	Billet B
Small	35.0	40.5
Large	37.5, 35.0	38.7, 39.5, 39.3

Within the limits of these data, again there is no evidence of a size effect nor of much dispersion among individual values, suggesting validity of the spurious-effect theory. It would appear that regardless of specimen size fracture occurs when the tensile stress at an internal pore reaches the following indicated value:

Billet A - 35.8 ± 3.6 ksi
Billet B - 39.5 ± 1.2 ksi
(95% confidence limits are shown)[6]

Accordingly, a simple maximum tensile stress criterion for strength also appears applicable to Pyroceram 9606 if the presence of internal pores must be taken into account.

An unobserved situation must be considered, however, in evaluating this criterion. Specifically, a "most-severe" flaw would be present if one of the 80-μm pores happened to lie immediately beneath a critical surface crack. Calculation of the fracture stress for this "worst" condition requires knowledge of the depth of critical surface cracks, and this depth can be estimated for Billet B material from data provided by Specimen BL-2. In this singular case, fracture initiated at a pore 30 μm in diameter located very near the surface (see Figure 9). Specimen BL-2 fractured at 55.5 ksi, while specimens from Billet B failing from a critical surface crack had an average strength of 57.1 ksi. Assuming that the pore in Specimen BL-2 acted like a surface crack 32 μm deep in intensifying stress, the inverse proportionality between strength and square root of crack depth (i.e., $\sigma_f \propto c^{-1/2}$) would apply and the depth of the critical surface crack would be

$$c = (55.5/57.1)^2 \times 32 = 30 \text{ μm}.$$

Thus, the "worst" condition would be a surface crack 30 + 80 = 110 μm deep, and the inverse proportionality relationship gives a stress of about 30 ksi for fracture from this surface crack. It follows that the conservative maximum tensile stress criterion is 30 ksi under the conditions of surface finish, strain rate, and environment used in these experiments. No failure would be expected if tensile stress is maintained below this value in a component of pore-containing Billet B material.

A similar approach was used to calculate the critical surface crack depth and then a "worst" condition fracture stress for Billet A material. The calculation was more complex than for the Billet B material, requiring that fracture energies be evaluated, and is described in the following section of this report. The calculation indicated that the critical surface crack is 40 μm deep making the "worst" condition a surface crack about 40 + 80 = 120 μm deep. For a crack this deep in Billet A material, fracture is calculated to occur at a stress of 26.0 ksi, which provides the conservative maximum tensile stress criterion for failure.

Our treatment of the data in Table 3 reveals that the strength of Pyroceram 9606 can be defined adequately in terms of stress alone; i.e., specimen size does not affect actual fracture stress. This finding would have been obscured by spurious effects if conventional strength-testing practice had been followed. In such practice, the larger values from surface origins and the smaller values from internal-pore origins would be averaged together in assigning a strength value. This strength value would exhibit a size effect because of the greater frequency of pore-site fractures among large specimens for reasons given previously, and consequently a lower strength value would be assigned to the large specimen. An off-setting error also would be present in the strength value because the maximum tensile stress rather than the actual stress at the fracture site is assessed in conventional bend testing. The error in each value is proportional to the distance of the fracture-origin site from the tensile surface, a distance that is a matter of chance in the case of pore-site failures. The off-setting error, of course, would occur more frequently in large than small specimens. In

addition to an apparent size dependence, these two spurious effects would cause data from conventional testing to exhibit a misleading dispersion among individual values. For purposes of academic interest, tabulated below are strength values reflecting these spurious effects obtained from the data in Table 3 by following conventional practice:

	Strength, ksi	
Specimen Size	Billet A	Billet B
Large	42.4 ± 6.5	49.5 ± 7.6
Small	43.4 ± 2.9	56.2 ± 3.2

Notes: (1) Data from specimens exhibiting edge-initiated fractures are not included in these average values. Had they been, values for large specimens would be smaller.

(2) 95 percent confidence limits are shown.[6]

It should be noted that the above tabulation shows an unreal size effect and misleading dispersions in strength values from known spurious effects even though precise stress measurements were made. In conventional testing, unknown errors from neglect of superposed stresses (e.g., friction, wedging, twisting, and unequal moments in bend tests and bending moments in direct tension tests) are usually present in the data. These errors would create further distortions in the assigned strength values.

Failure Criterion for Billet A Material

The following generalized Griffith-Orowan expression was used to calculate the fracture stress in Billet A material for the condition of a 80-μm internal pore immediately below a critical surface crack:

$$\sigma_f = A(\gamma_f E/c)^{1/2} \qquad (1)$$

In using this relationship, A, the geometric factor, is assumed to have a different value for internal-pore and surface failure origins (A_p and A_s), but to be independent of the material. The fracture energy, γ_f, however, is assumed different for Billet A and B materials, γ_{fA} and γ_{fB}. Young's modulus, E, was measured and found to have the same value, 16.6×10^6 psi, for both materials. The term, c, in the above expression is either the surface crack depth, c_s, or the "effective" radius of an 80-μm internal pore, c_p, depending on which was found at the fracture origin. The value of c_s, of course, is different in A and B materials (c_{sA} and c_{sB}), but c_p is assumed the same for the observed pore failure origins in both materials since the pores in the two were indistinguishable.

Data provided by Specimen BL-2 permit a calculation of fracture energy, γ_{fB}, for Billet B material, using the following exact form of the above equation:[7]

$$\sigma_{fB} = [\pi E \gamma_f / 2c_{sB}(1-\nu^2)]^{1/2} \qquad (2)$$

where: σ_{fB} = fracture stress = 55.5 ksi

E = Young's modulus = 16.6×10^6 psi

c_{sB} = crack depth = 32 μm

ν = Poisson's ratio = 0.245*

---

* Value from Corning's Data Sheet on Pyroceram 9606.

The value of fracture energy so obtained is 24.5 J/m2 which is in close agreement with the value of 22.5 J/m2 measured by McKinney and Smith[8] on precracked specimens of Pyroceram 9606.

Using the value 24.5 J/m2 for γ_{fB}, and the measured values σ_{fA} and σ_{fB} = 35.8 and 39.5 ksi for the internal-pore fracture stresses, the following relationships * are obtained from Equation (1):

$$\text{Billet B} \qquad 39.5 = A_p \, (24.5 \times E/c_p)^{1/2}$$

$$\text{Billet A} \qquad 35.8 = A_p \, (\gamma_{fA} \times E/c_p)^{1/2}$$

From these relationships, $\gamma_{fA} = 24.5 \, (35.8/39.5)^2 = 20.1$ J/m2.

The critical surface crack depth for Billet A material can now be evaluated from the following relationships * also obtained from the generalized expression, Equation (1), and the measured values, σ_{fB} = 57.1 ksi and σ_{fA} = 45.0 ksi:

$$\text{Billet B} \qquad 57.1 = A_s \, (24.5 \times E/30)^{1/2}$$

$$\text{Billet A} \qquad 45.0 = A_s \, (20.1 \, E/c_{sA})^{1/2}$$

From these relationships, the depth of the critical surface crack in Billet A material, $c_{sA} = 30 \times 20.1/24.5 \, (57.1/45.0)^2 = 40$ μm.

---

* In inconsistent units.

The "worst" condition in A material, therefore, is a surface crack approximately 40 + 80 = 120 μm deep. From Equation (2), a surface crack this deep would result in fracture at a stress of 26.0 ksi. This value is considered to be the conservative maximum tensile stress criterion for failure of Billet A material.

FUTURE WORK

Project plans for the immediate future will feature effort directed to obtaining similar precise strength data for Pyroceram 9606 under controlled environmental and strain-rate conditions favoring subcritical crack growth and with minimum stored strain energy in the loading apparatus, for three reasons:

(1) The material will be subjected to conditions favoring subcritical crack growth in practical applications.

(2) The surface fracture stress should be lowered, but the internal pore fracture stress should be unaffected. Therefore, the presence of pores should become a less significant factor in strength, and may not require consideration in developing a fracture criterion for design use.

(3) By maximizing the energy dissipated by the fracture event relative to the total stored strain energy in the material, predictions of the stored-strain-energy theory may hold and a size dependence of strength for this reason may be observed.

Future plans also include strength measurements in direct tension and on specimens of smaller size to determine whether the same failure criterion applies to these extended experimental conditions.

Also, microstructures of Billet A and Billet B materials will be more thoroughly characterized in an effort to explain the observed differences in their strength levels.

A similar investigation and analysis of strength-size relations exhibited by a high-Al_2O_3 ceramic has been started and will be completed in future project work.

REFERENCES

(1) Weibull, W., "A Statistical Theory of the Strength of Materials", Ing. Ventenskaps Akard Handl., No. 151, Stockholm (1939).

(2) Berenbaum, R., and Brodie, I., "Measurements of the Tensile Strength of Brittle Materials", Brit. J. Appl. Phys., 10, 281-287 (1959).

(3) Glucklich, J., "Strain Energy Size Effect", Jet Propulsion Laboratory Tech. Rep. 32-1438 (August, 1970).

(4) McMillan, P. W., Glass-Ceramics, Academic Press, London & New York (1964).

(5) Hoagland, R. G., Marschall, C. W., and Duckworth, W. H., Battelle's Columbus Laboratories, "Reduction of Errors in Ceramic Bend Tests", Tech. Rep. 1, Office of Naval Research, Contract No. N00014-73-C-0408, NR 032-541, (July, 1974).

(6) ASTM Manual on Quality Control of Materials, Special Technical Publication No. 15-C (January, 1951).

(7) Davidge, R. W., and Evans, A. G., "The Strength of Ceramics", Mater. Sci. Eng., 6, 281-298 (1970).

(8) McKinney, K. R., and Smith, H. L., "Method of Studying Subcritical Cracking of Opaque Materials", J. Am. Ceram. Soc., 56 (1), 30-32 (1973).